

# BALLISTIC RESISTANT ANALYSIS FOR AIRCRAFT WING STRUCTURE

Guangran Zu, Yang Pei, Xiaowu Yang

School of Aeronautics, Northwestern Polytechnical University, Xi'an Shaanxi, China

**Keywords:** *Ballistic resistant design, warhead power field, aircraft wing structure, damage model*

## Abstract

*In the paper, numerical simulations of an aircraft wing structure are performed to study its ballistic resistant ability with the dynamic simulation method. For military aircraft wing structure models, finite element model is established and compared with experiment for the purpose of improving aircraft design and structure survivability chances in a survival accident. It is found that a reasonable weakness setting on the wing structure and elastic are advantageous in the energy absorption during the impact process. Meanwhile, the impact load is on the most severe level in all damage data which can be measured by the wing surface deformation efficiency and reducing is better to decrease the vulnerability. At last, the paper imposes some measures and ideas to improve the aircraft wing structure ballistic resistant ability.*

## 1 Introduction

Improving the combat aircraft survivability is a growing concern for aircraft designers and customers [1]. One of the key problems is to analyze the degree to which the threat element damages various parts of the aircraft. According to the analysis results, minimize the damage degree of the aircraft which based on the basic design principles, i.e. the aircraft vulnerability reduction design.

The non-explosive projectile and missile warhead are the major threat to aircraft. The research on aircraft high survivability design measures of conventional threat elements has received extensive attention from the military and scholars of major military power. The

Technological Application Program Office (TAPO) [2] has designed a ballistic protection system for aircraft crew aiming at reducing the vulnerability of them. Torger et al. [3] assessed the survivability of aircraft crews when they was hit, and imposed some measures. Besides, The Joint aircraft survivability program office [4] imposes the vulnerability reduction of structures and materials each year, that's the reliable reference of vulnerability research trend.

As one of the major parts of aircraft, aircraft wings not only affects the aerodynamic performance of aircraft, but bears various loads from outside. In the analysis of aircraft survivability, the wing is the part with the largest exposure area of aircraft. Therefore, it is particularly important to analyze the ballistic resistant ability of aircraft wings and propose corresponding measures. It is meaningful, in other words, to study the ballistic resistant design for improving the aircraft wings combat survivability and sustainability.

The paper make the anti-air missile warhead as the threat element, the fix-wing fighter as the object. In section 2, the paper studies anti-aircraft missile warhead power field which is used to describe missile kill target capability. The aircraft wing structure model is established in section 3. Besides, the simulation procedures are described in section 4. Then, we provide a further damage analysis of the aircraft wing structure in section 5. At last, some ballistic resistant design measures and ideas are proposed to improve the aircraft wing structure by comparing the kinds of damage indicators.

## 2 Establishment of anti-aircraft missile warhead power field model

$$K_d = \frac{C_s \rho A}{2m} \quad (4)$$

The concept of anti-aircraft missile warhead power field was imported to establish one of important model of analysis for aircraft wing structure. The basic concept and character of power field was brought forward and effective factors was analyzed. The power field model of anti-aircraft missile warhead includes fragment power field and blast wave power field.

## 2.1 The modeling principles of fragment power field

The effective fragments produced by warhead explosion can kill the aircraft target. According to the damage mechanism, the fragment power field model parameters are divided into two categories: fragment speed series and flying parameters series. The fragment speed parameters series include the initial velocity of fragment, the attenuation coefficient and the distribution of fragment. The flying parameters series mainly indicates the angle of splashing fragment.

### 2.1.1 The initial velocity of fragment

The initial velocity of fragment refers to the maximum velocity after receiving the energy transferred by the explosive detonation product. Gurney formula is usually used to calculate the parameter as Eq. (1)

$$v_0 = \sqrt{2E} \sqrt{\frac{\beta}{1 + \beta/2}} \quad (1)$$

Where,  $\sqrt{2E}$  is gurney constant,  $\beta$  is the charge-weight ratio of the warhead. Its definition equation as Eq. (2).

$$\beta = C/M \quad (2)$$

### 2.1.2 The velocity attenuation coefficient

When the initial velocity of fragment and dispersion distance  $s$  are known, the residual velocity of the fragment is shown as Eq. (3).

$$v = v_0 e^{-K_d s} \quad (3)$$

where,  $K_d$  is the velocity attenuation coefficient of fragment. Its definition equation is shown as Eq. (4).

In Eq. (4),  $C_s$  is shape factor.  $\rho$  is the density of fragment.  $A$  is windward area of fragment,  $m$  is the fragment mass.

### 2.1.3 The distribution of fragment

In the process of analysis, the deflection angle of each fragment is different due to the location of each fragment from the starting point. The statistical standard of the distribution of fragment is that the cone angle of the effective fragment is not less than 90% in the flying plane. According to the actual situation, it is necessary to conclude by FEM simulation.

### 2.1.4 The angle of splashing fragment

The angle of splashing fragment is another important parameter in the process of analysis. The endpoint is the center of mass of warhead. Then, we make a parallel plane along the axis of warhead. Hence, the flying angle can be defined that a certain cone angle as required.

## 2.2 The modeling principles of blast wave power field

The damage form of blast wave to the aircraft wing structure is destruction. Its damage mechanism includes specific impulse and peak overpressure.

### 2.2.1 The specific impulse principle of blast wave

According to damage mechanism, when the blast wave reaches or exceeds a minimum critical specific impulse at a critical time, the target structure can be identified damaged. That is to say, the reference point of specific impulse is an amplitude.

### 2.2.2 The peak overpressure principle of blast wave

The peak overpressure principle of blast wave is similar to the specific impulse. If a structure is considered to be damaged, the peak overpressure should exceed a critical number, and the duration time needs a certain standard. Only meet the above principle, the blast wave can cause a given damage to the target structure.

## 2.3 Anti-air missile warhead power field models details

### 2.3.1 The basic parameters of target warhead

The target warhead shape is cylindrical. Its total length is 18.5cm. No.8701 is selected for warhead charging explosive material. The charging radius is 5cm. Steel alloy is chosen for the inner lining and shell, the thickness of the two parts is 0.5cm and 1.5cm respectively. The killing element chooses the ball-shaped precast fragment. Each fragment has a diameter of 6.35cm. The total number of fragment is 468. The warhead is fired from the center. The warhead structure which according to the above condition is shown in Fig.1

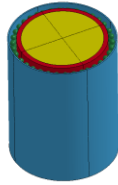


Fig.1 The structure of target warhead

### 2.3.2 The parameters of target warhead

The parameters of target warhead can be categories into 2 parts: the material mechanical properties and the constitutive properties. Related data are shown as Table.1 to Table. .

Table.1 Material mechanical properties of explosive of target warhead

Parameters	Values
Density	1.787
Detonation velocity	1.500
Pressure	0.34
Constant A	5.814
Constant B	$6.801 \times 10^{-2}$
Constant $R_1$	4.1
Constant $R_2$	1.0
Constant $\omega$	0.35
Initial per volume	0.09
The initial relative volume of the explosive	1.0

Table.2 Material mechanical properties of shell of target warhead

Parameters	Values
density	7.83
shear modulus	0.77
yield stress constant A	$7.92 \times 10^{-3}$
strain harden constant B	$5.1 \times 10^{-3}$
strain harden index n	0.26

strain rate coefficient index C	0.014
melting temperature $T_{mell}$	1793
room temperature $T_{room}$	294
temperature correlation index	1.03
sound velocity c	0.4578
first slope coefficient $S_1$	1.49
second slope coefficient $S_2$	0
third slop coefficient $S_3$	0
Gruneisen index	2.17
first order correction factor of $\gamma_0$	0.46
initial energy	0

Table.3 Material mechanical properties of controlled fragment of target warhead

Parameters	Values
Density	17.8
elasticity modulus	$3.23 \times 10^{-5}$
Poisson ratio	0.22

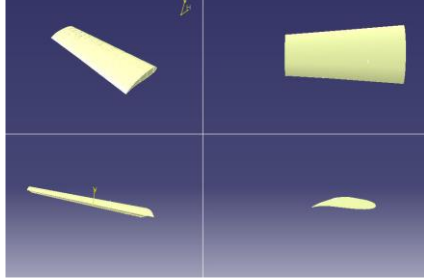
Table.4 Material mechanical properties of lining of target warhead

Parameters	Values
density	7.83
shear modulus	0.77
yield stress constant A	$7.92 \times 10^{-3}$
strain harden constant B	$5.1 \times 10^{-3}$
strain harden index n	0.26
strain rate coefficient index C	0.014
melting temperature $T_{mell}$	1793
room temperature $T_{room}$	294
temperature correlation index	1.03
sound velocity c	0.4578
first slope coefficient $S_1$	1.49
second slope coefficient $S_2$	0
third slop coefficient $S_3$	0
Gruneisen index	2.17
first order correction factor of $\gamma_0$	0.46
initial energy	0

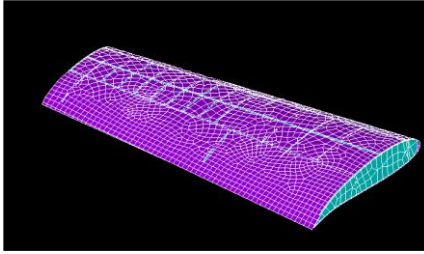
## 3 Establishment of aircraft wing model

The paper selects attacker as the research object. Attack plane usually carry out close air support and other high-risk combat missions. Therefore,

it is of great significance to study the survivability of attack plane. In this paper, a typical attack plane wing is selected as the research model. The 3-D digital model and FEM model is shown as Fig.5. The shape parameters of aircraft wing is shown as Table.2.



(a)



(b)

Fig.2 The model of attack plane wing  
(a) The 3-D digital model (b) The FEM model

Table.5 the shape parameters of wing model

Parameter type	Parameter value
span length	17.53m
wing surface area	47m <sup>2</sup>
root chord	3.04m
tip chord	1.99m
average chord	2.73m
span-chord ratio	6.54
wing profile type	NACA 6716
material	Al-2024-T3 Al-7075-T6

The Al-2024-T3, Al-7075-T6 are used in the wing surface section with the linear elastic-plastic constitutive model and strain failure criterion. Material mechanical properties are shown in Table.6.

Table.6 Mechanical properties of the wing surface section

material	Al-2024-T3	Al-7075-T6
Elastic Modulus	66.3	71.0
Poisson's ratio	0.33	0.33
Density	2.796	2.768
Yield modulus	243	362
Strengthening modulus	826	1001
Failure strain	0.14	0.045

Due to the large deformation in damage process, Johnson-Cook constitutive model was selected for the wing. The model definition equation is shown as Eq. (5)

$$\sigma_y = \left( A + B(\varepsilon^p)^n \right) \left( 1 + C \ln \left[ \frac{\varepsilon^p}{\varepsilon^0} \right] \right) (1 - T^m) \quad (5)$$

Material constant(A、B、C、m、n) are determined by different types of materials.  $T^m$  is the temperature coefficient. The related parameter values are shown in Table. where,  $D_1 \sim D_5$  are the material failure parameters,  $\rho$  is density,  $G$  is shear modulus,  $A$  is yield stress constant,  $B$  and  $n$  is strain hardening constant,  $m$  is temperature correlation coefficient,  $C$  is strain rate correlation coefficient,  $T_m$  is melting temperature,  $T_r$  is room temperature,  $EPSO$  is rate normalization factor,  $C_p$  is specific heat,  $P_C$  is truncation pressure,  $SPALL$  is fatigue type,  $IT$  is plastic strain option. The specific meaning of

the above parameters can be found in Ref. [3]. All values of parameters in this section comes from Ref. [4].

Table.4 Main parameters of Johnson-Cook constitutive model

material	Al-2024-T3	Al-7075-T6
$D_1$	0.112	0.112
$D_2$	0.123	0.123
$D_3$	1.500	1.500
$D_4$	0.007	0.007
$D_5$	0.000	0.000
$\rho$	17.8	17.8
$G$	1.37	1.37
$A$	53.517	53.517
$B$	99.202	99.202
$m$	1.7	1.7
$n$	0.73	0.73
$C$	0.0083	0.0083
$T_m$	1498	1498

$T_r$	293	293
EPSO	1.0E-06	1.0E-06
$C_p$	1.35E-06	1.35E-06
$P_C$	-1.75	-1.75
SPALL	2.0	2.0
IT	0	0

The state equation of wing model is *Gruneisen* equation as follows:

$$P = \frac{\rho_0 c^2 \mu \left[ 1 + \left( 1 - \frac{\gamma_0}{2} \right) \mu - \left( \frac{a}{2} \right) \mu^2 \right]}{\left[ 1 - (S_1 - 1) \mu - S_2 \frac{\mu^2}{\mu + 1} - S_3 \frac{\mu^3}{(\mu + 1)^2} \right]^2} + (\gamma_0 + a\mu) E \quad (6)$$

#### 4 Numerical simulation

Currently, the damage experiment is the most trusted method to analysis and evaluate the aircraft wing structure ballistic resistant ability, but experiment make the analysis and design cycle so long and costly that unaffordable to research institution. Hence, high precision simulation method and model can significantly overcome the above disadvantages.

Firstly, the 3-D digital model is established in modeling software. Then, the model is imported in ANSYS/LS-DYNA [5] to be meshed and generated the K file. The K file is submitted to LS-DYNA Solver and output related results after the former steps. The procedure is shown in the Fig. 3.

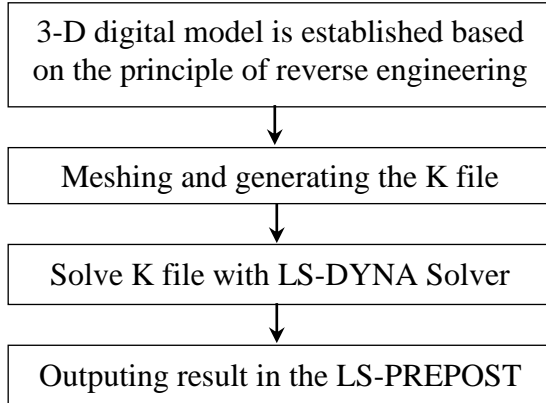


Fig.3 The flowchart of FEM simulation analysis in the paper

A certain type model of aircraft which is refer to A-10 attacker is taken as the study object which contains 3 parts: surface, spar, rib. The finite element models of all the components are shown in Fig.2.

The contact type between fragment and wing skin in surface to surface contact, between

fragments and wing structure components is node to surface contact, the dynamic friction factor of both contact is 0.1 and the static friction factor is 0.2.

#### 5 Result and discussion

In this section, three aspects, including different target angles, different strike positions and different hit heights, are analyzed respectively. Then, the stress changes of the wing surface structure under the hit of fragmentation are studied. Combining the experiments with results of calculation, we described the damage degree of wing surface structure. Finally, the ability and measures to anti-fragment kill was discussed.

##### 5.1 Damage from different angles

In this sub-section, the damage degree of wing surface and structure by warhead is studied from  $90^\circ$ ,  $45^\circ$ ,  $30^\circ$  and  $0^\circ$ . Von-mises criterion is taken as the measurement standard. The images and analysis results from different attack situation are shown in Fig.4 and Fig.5.

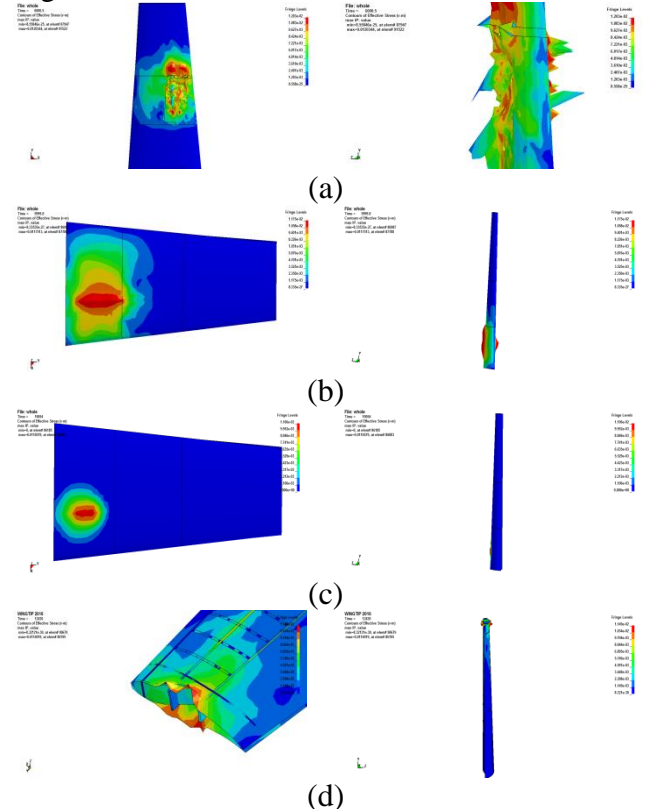


Fig.4 The damage and deformation of aircraft wing:



(a)  $90^\circ$  ;(b) $45^\circ$  ;(c) $30^\circ$  ;(d) $0^\circ$

Fig.4-(a) reflects the images of fragments hit the wing structure from  $90^\circ$  . As can be seen from the illustration, the high density part of fragments can make petal perforation in the wing surface. The perforated area in upper surface is greater than lower surface. Fig.4-(b) reflects the images of fragments hit the wing structure from  $45^\circ$  . The phenomenon is different from the vertical strike. As can be seen, the form of hole in wing surface is banding uplift. The penetration is not obvious than the former situation. Fig.4-(c) reflects the images of fragments hit the wing structure from  $30^\circ$  . Although the phenomenon is similar to Fig.4-(b), the damage area is lower. The lower wing surface is not damaged. Fig.4-(d) reflects the images of fragments hit the wing structure from  $0^\circ$  . At this situation, petal failure phenomenon occurs on the tip of wing, The rib in tip position exceeds the yield limit. That is, the structure is unstable.

Through calculate the case of damage by the fragments in  $90^\circ$  ,  $45^\circ$  ,  $30^\circ$  and  $0^\circ$  on the surface. According to the image, we can obtain different damage conditions of the wing structure. The following is an analysis of the wing structure failure condition from different angles.

1. From the perspective of the residual velocity of the fragment when the surface is penetrated by the fragment in four states. When fragments penetrate the wing surface, as for the difference of the damage Angle, under the condition of the same height (distance) blow, the smaller the Angle, the less fragment quantity to reach the aircraft wing surface. The fragments hit the area shows a trend of narrow. Besides, because the detonation product energy constantly release to fragment, the velocity of the fragment keeps increasing, but when it comes into contact with the wing surface and begins the penetration process, the velocity of the fragment tends to be stable. This means that the damage ability from fragment to the wing is reduced.

2. In four cases, we choose the typical element with the greatest degree of damage. As can be seen from Fig. 5. With the increasing

number of cracks in a certain area, the stress value of the wing surface increases in a wave-like manner. When the stress is up to 670MPa, failure will occur on the wing surface. And it will break into petal shape. As a result of the transfer of stress waves within the wing, when the part of the wing reaches 443 MPa, the wing surface will break. However, the number of fragments accumulated in vertical strike is more than that of angular strike. So although the same stress conditions, the extent of the damage of the wing surface of  $90^\circ > 45^\circ > 30^\circ > 0^\circ$  . According to the comparison with the data and the trend shown in literature [6] when the real aircraft wings strike from the above angles, the simulation results are consistent with the experimental results of the real aircraft wing strike.

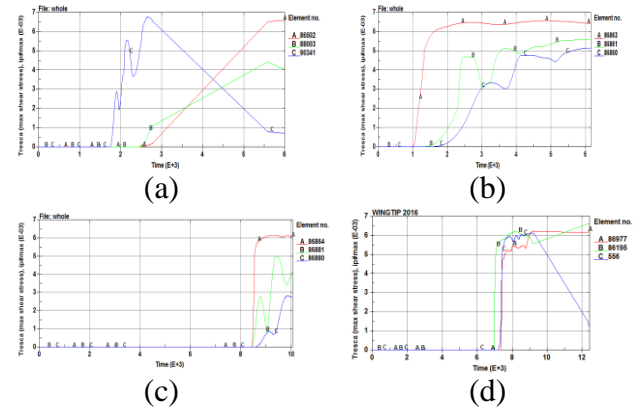


Fig.5 The typical element damage stress-time images of aircraft wing:  
(a)  $90^\circ$  ;(b) $45^\circ$  ;(c) $30^\circ$  ;(d) $0^\circ$

3. The damage form of the fragment to the wing surface and the inner structure is different. As for the thickness of the wing skin is different from that of the bearing structure. Therefore, in the same case of being hit by the fragment, the skin was seriously damaged, and the location of the fragment accumulation caused partial accumulation and wrinkling of the skin. Fracture damage is greater. However, the damage to the wing structure first produces buckling, and with the increase of the number of cracks in the wing structure, the structure is finally broken and failed due to perforation. Such as warhead hit from the wing tips, according to the simulation image and Fig.4 as you can see, when in  $9140\mu s$  reach the yield limit of 1030 MPa, after when the wing handle

more than 1030 MPa and continues after a period of time due to fracture, the residual strength is not enough to support the wings continue bearing structure.

## 5.2 Damage from different positions

In this sub-section, the damage position of wing surface and structure by warhead is studied from wing root, wing tip and middle of wing. Von-mises criterion is also taken as the measurement standard. The images and analysis results from different attack situation are shown in Fig.6 and Fig.7.

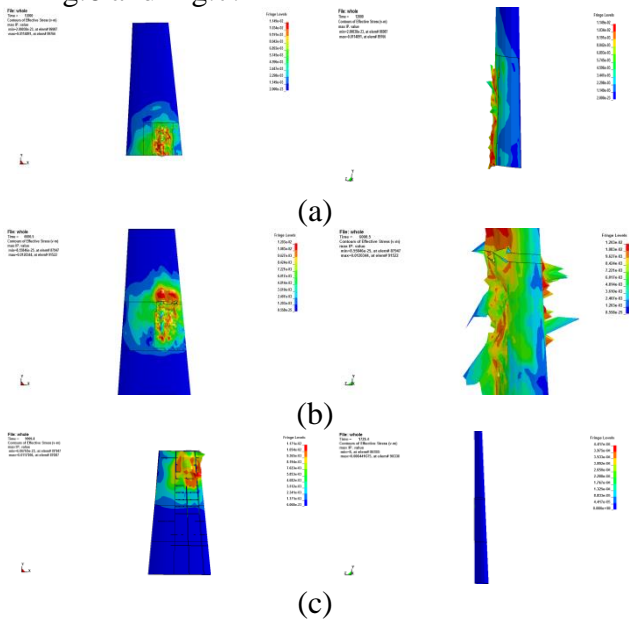


Fig.6 The damage and deformation of aircraft wing:  
(a) Wing root (b) middle of wing (c) wing tip

Through the damage situation was calculated in the central wing, pointed, the wings and wing root three cases from the fragment hit surface of the wing, according to the image can be obtained in the different situation to offload carefully mutilate form below. In these three cases, the stress cloud map of the damaged part of the wing, namely Fig.6 was selected, and the typical unit with the greatest damage degree was analyzed. As can be seen from Fig.7. At the same height and at different positions, the cautious plane is struck. The wing root is the part with the largest area of the damaged wing surface and the widest stress propagation in the wing surface. Because the wing root is connected to the fuselage. The damage was caused by a beam in the middle of

the wing. It can be seen from the curve diagram of equivalent stress at the root of the beam in fig.6 that the partial stress of the beam has exceeded the yield limit of the material. Therefore, it can be concluded that the root of the entire surface of the wing is the most dangerous section. The energy density is higher than that of the rest of the wing because the area of the wing tip is smaller than that of the wing root. There are more pieces of the inner structure of the wing that can be damaged. However, only 2 ribs in the middle section of the wing are damaged. Therefore, the degree of damage to the wing gingerly surface is in turn root > tip > middle of wing.

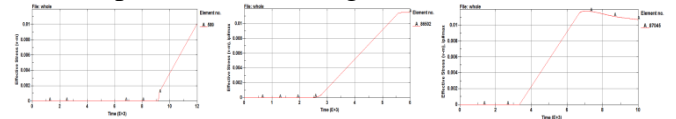
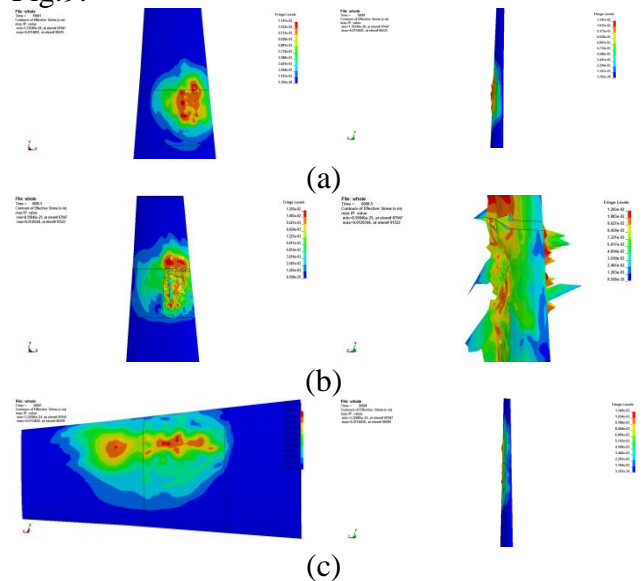


Fig.7 The typical element damage stress-time  
images of aircraft wing:  
(a) root (b) middle of wing (c) wing tip

## 5.3 Damage from different heights

In this sub-section, the damage height of wing surface and structure by warhead is studied from 3m, 5m, 10m and 15m. Von-mises criterion is also taken as the measurement standard. The images and analysis results from different attack situation are shown in Fig.8 and Fig.9.



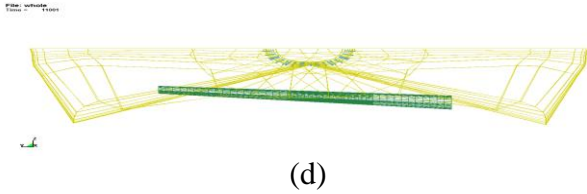


Fig.8 The damage and deformation of aircraft wing:  
(a) 3m (b) 5m (c) 10m (d) 15m

According to the above situation that the warhead at different height has damaged the aircraft's wing surface, it can be seen that the height of different explosion points has a direct impact on the degree of wing damage and the regional influence. From the results, when the vertical distance  $h$  between 0m and 15m, the blast point and wing in the warhead fragment can cause direct damage to the wing, damage area with distance increases with the increase slightly, but as the distance increases with the reduction in damage, and the degree of attenuation is obvious. When distance above 15 m, because the shock waves arrive prematurely wing before fragment, the fragment to the situation of airplane wing surface damage can be neglected, and the shock wave damage degree is far lower than the fragment of the wing, so can be regarded as the wing damage degree is low.

## 6 Conclusions

In this paper, according to the aircraft vulnerability assessment and design principles, the ballistic resistant ability of aircraft wing structure is evaluated and analyzed by numerical simulations and gets following conclusions:

1. For the aircraft wing shape design, the designer should lower the impact angle (The angle is between the tangent direction of the outer surface of the structure and the direction of flight) as far as possible. Meanwhile, the wing root structure should be strengthened. These actions can reduce the vector component of ballistic impact load.

2. The aircraft wing structure should consider increasing the energy absorption characteristic and dissipative energy characteristic. The purpose is to ensure structure

can fully absorb or dissipate impact energy from the warhead fragment and blast wave.

3. The multilayer protection design should be used in critical areas. The main reason for this design method is to reduce disruptive behavior and damage degree through the layered absorption.

## References

- [1] R.E. Ball. *The fundamentals of aircraft combat survivability analysis and design*. 2st edition, AIAA, 2002.
- [2] Derek B, Caroline M, Michael S. et, al. Improving special operations aircraft survivability through better ballistic protection systems. *Proceedings of the 2009 IEEE Systems and information engineering design symposium*, University of Virginia, Vol.1 pp153-157, 2009.
- [3] Torger A, Joel W., and Leonard F. Vulnerability reduction features for commercial derivative combat aircraft. *47<sup>th</sup> AIAA/ASME/ASCE/AHS/ASC structures, structural dynamics and materials and co-located conference*. AIAA, Vol.1 pp.7-11, 2006.
- [4] Michael R., Update on the Joint Aircraft Survivability Program(JASP) , *51<sup>st</sup> AIAA/ASME/ASCE/AHS/ASC structures, structural dynamics and materials conference*, AIAA, Florida, pp1-9, 2010
- [5] Anon., LS-DYNA3D User's Manual, Livermore Software Technology Company, Livermore, CA, 1997.
- [6] Q. Dong, Damage analysis of wing perforated skin under explosive shockwave. *Machine Building & automation*, Vol.42, pp 46-48, 2013.

## Acknowledgement

The authors gratefully acknowledge the support from National Natural Science Foundation of China (No.11472214) and Aeronautical Science Foundation of China (No.20174123008).

## Contact Author Email Address

Contact Author: YANG PEI  
mailto: peiyang\_yang@nwpu.edu.cn



### **Copyright Statement**

The authors confirm that they, and/or their company or organization, hold copyright on all of the original material included in this paper. The authors also confirm that they have obtained permission, from the copyright holder of any third party material included in this paper, to publish it as part of their paper. The authors confirm that they give permission, or have obtained permission from the copyright holder of this paper, for the publication and distribution of this paper as part of the ICAS proceedings or as individual off-prints from the proceedings.